Stiffness-dependent cellular internalization of matrix-bound BMP-2 and its relation to Smad and non-Smad signaling

Flora Gilde[1,2,#], **Laure Fourel**[3,4,5,#], **Raphael Guillot**[1,2], **Isabelle Pignot-Paintrand**[1,2], **Takaharu Okada**[6], **Vincent Fitzpatrick**[1,2], **Thomas Boudou**[1,2], **Corinne Albiges-Rizo**[3,*], and **Catherine Picart**[1,2,*]

[1]CNRS UMR 5628 (LMGP), MINATEC, 3 parvis Louis Néel, 38016, Grenoble, France

[2]Université Grenoble Alpes, Grenoble Institute of Technology, 3 parvis Louis Néel, 38016, Grenoble, France

[3]INSERM U1209, Institut Albert Bonniot, Site Santé, BP170, 38042 Grenoble cedex 9, France

[4]CNRS UMR5309, Institut Albert Bonniot, Site Santé, BP170, 38042 Grenoble cedex 9, France

[5]Université Grenoble Alpes, Institut Albert Bonniot, Institute of Advanced Biosciences, Site Santé, BP170, 38042 Grenoble cedex 9, France

[6]Biomaterials Unit, International Center for Materials Nanoarchitectonics (WPI-MANA), National Institute for Materials Science (NIMS), 1-1 Namiki, Tsukuba, Ibaraki 305-0044, Japan

Abstract

Surface coatings delivering BMP are a promising approach to render biomaterials osteoinductive. In contrast to soluble BMPs which can interact with their receptors at the dorsal side of the cell, BMPs presented as insoluble cue physically bound to a biomimetic matrix, called here matrix-bound (bBMP-2), are presented to cells by their ventral side. To date, BMP-2 internalization and signaling studies in cell biology have always been performed by adding soluble (sBMP-2) to cells adhered on cell culture plates or glass slides, which will be considered here as a "reference" condition. However, whether and how matrix-bound BMP-2 can be internalized by cells and its relation to canonical (SMAD) and non-canonical signaling (ALP) remain open questions. In this study, we investigated the uptake and processing of BMP-2 by C2C12 myoblasts. This BMP-2 was presented either embedded in polyelectrolyte multilayer films (matrix-bound presentation) or as soluble form. Using fluorescently-labeled BMP-2, we showed that the amount of matrix-bound BMP-2 internalized is dependent on the level of crosslinking of the polyelectrolyte films. Cav-1-mediated internalization is related to both SMAD and ALP signaling, while clathrin-mediated is only related to ALP signaling. BMP-2 internalization was independent on the presentation mode (sBMP-2 versus bBMP-2) for low crosslinked films (soft, EDC10) in striking contrast to high crosslinked (stiff, EDC70) films where internalization was much lower and slower for bBMP-2. As anticipated, internalization of sBMP-2 barely depended on the underlying matrix. Taken together, these results indicate that BMP-2 internalization can be tuned by the underlying matrix

[*]Corresponding authors: catherine.picart@grenoble-inp.fr, Corinne.albiges-rizo@ujf-grenoble.fr.
[#]co-first authors

and activates downstream BMP-2 signaling, which is key for the effective formation of bone tissue.

1   Introduction

The bone morphogenetic proteins (BMPs) are members of the transforming growth factor-β (TGF-β) family [1] and play important roles in a large number of physiological and pathological processes [2, 3]. BMP-2 is a highly potent morphogen that induces the differentiation of mesenchymal stem cells as well as muscle satellite cells into bone cells [4–6]. In terms of signaling, the BMP-2 ligand may bind directly to preformed receptor complexes [7, 8] composed of BMPR-I and II before activating either Smad (canonical) or Smad-independent (non-canonical) pathways [9] [10]. One of the markers for the non-canonical pathway is the induction of alkaline phosphatase (ALP) [9] [11].

BMP-2 has been used in orthopedic clinical practice for the treatment of spinal fusion and non-unions [12] with a formulation using a type I collagen sponge which is soaked in a solution of BMP-2 at a very high dose. This has raised growing concerns about the uncontrolled release of BMP-2 and its possible side effects, including heterotopic ossifications and immunological reactions [13]. The spatially-controlled administration of lower doses of BMP-2 from implantable materials could broaden their clinical use.

In the body, BMPs exist in matrix-bound forms [14]. Mimics of the natural extracellular matrix [15], including fibrin films [16, 17], alginate [18, 19] and hyaluronan (HA) hydrogels [20] [21], or biopolymer-based layer-by-layer films [22, 23] appear particularly interesting as carriers for BMP-2 in view of their affinity for BMP-2, which enables an enhanced retention and localized delivery.

We recently showed that poly(L-lysine) (PLL) and hyaluronan (PLL/HA) multilayer films can be used as an efficient carrier of BMP-2 [22] and are osteoinductive *in vivo* when deposited on ceramic granules [24] and titanium implants [25]. The BMP-2-loaded films were found to preserve the secondary structure of BMP-2 in comparison to its conformation in solution at acidic pH [26]. In addition, bBMP-2 was also found to trigger cell spreading, migration, and the formation of focal adhesions, especially when matrix-bound BMP-2 was delivered from a weakly crosslinked film [27]. Our recent studies also revealed that matrix-bound BMP-2 presented from a highly crosslinked film increased the dynamics of focal adhesions, as assessed by GFP-paxillin recruitment, when compared to soluble BMP-2 [28].

However, whether and how matrix-bound BMP-2 can be internalized by cells and its relation to canonical and non-canonical signaling remain open questions. In this study, we investigated (i) the ability of matrix-bound BMP-2 to be internalized by cells, (ii) the role of the crosslinking level of the biomaterial in the BMP-2 internalization process and (iii) the coupling between BMP-2 endocytosis and signaling. To this end, we have monitored the

delivery of matrix-bound BMP-2 using fluorescently labeled BMP-2 as a function of the crosslinking level of polyelectrolyte films. In view of the fact that all endocytosis studies so far have been done by cell biologists, using soluble BMP-2 as a bioactive trigger [29], we also included sBMP-2 as a "reference" condition. Using a pharmacological approach and a gene silencing strategy, we showed that Smad and ALP signaling are regulated by different routes.

2   Experimental section

2.1   Polyelectrolyte multilayer (PEM) film buildup, BMP-2 loading and film characterization by infrared spectroscopy

PEM deposition was performed using poly(L-lysine) hydrobromide (PLL, P2626, 6.8×10^4 g/mol, Sigma) at 0.5 mg/mL, and hyaluronic acid (HA, 360 kDa, Lifecore, USA) at 1 mg/mL dissolved in a Hepes-NaCl buffer (0.15 M NaCl, 20 mMHepes pH 7.4). The $(PLL/HA)_{24}$ film (i.e. film made of 24 layer pairs) buildup using an automated dipping machine (Dipping Robot DR3, Kierstein GmbH, Germany) and the subsequent crosslinking were done as previously described [22].Three concentrations of the 1-Ethyl-3-(3-Dimethylamino-propyl) carbodiimide (EDC) crosslinker, namely EDC10, 30 and 70 were used (corresponding to 10, 30 and 70 mg/mL of EDC). BMP-2 was loaded at 20 μg/mL in the crosslinked $(PLL/HA)_{24}$ films by post-diffusion of the protein in 1 mM HCl [22]. The BMP-2-loaded films were thoroughly washed in the Hepes-NaCl buffer to remove any loosely-bound BMP-2 and to present BMP-2 exclusively in a matrix-bound manner to the cells. This mode of presentation will be named hereafter bBMP-2 in comparison to the presentation of soluble BMP-2 (sBMP-2) considered here as a control. It is worth mentioning that we adopted the terminology "matrix-bound presentation", which is also sometimes referred to as "insoluble" [30] for the sake of continuity with our previously published articles [22]. For confocal observation, BMP-2 labeled with carboxyfluorescein (BMP-2^{CF},21878, Sigma) was used [22], as well as PLL labeled with Alexa Fluor®568 (A568, A20003 Life Technologies).

The effect of a pH change on the secondary structure of (PLL/HA) films was assessed by FTIR spectroscopy. To this end, films were built and crosslinked on a silicon wafer as previously described [26]. The spectra of $(PLL/HA)_{12}$ films were acquired after film were prepared in HEPES-NaCl at pH 7.4, then rinsed at pH 3 with HCl 1 mM and finally rinsed again in HEPES-NaCl at pH 7.4. All solutions were prepared in H_2O. The subtraction between the different spectra evidenced structural changes due to pH variations during the process of BMP-2 loading.

2.2   Immunogold labeling of BMP-2

Films were built on Thermanox® slides, crosslinked and loaded with BMP-2 as described above. The sample was fixed with 2.5 % glutaraldehyde in 0.1M sodium cacodylate (C0250, Sigma) buffer, pH 7.2). Then, a post-fixation with 1% osmium tetroxide (ref 75632, Sigma) and 1.5% potassium hexacyanoferrate (II) trihydrate (P9387, Sigma) was performed. The sample was then dehydrated with an ethanol dilution series and embedded in HM20 resin (14345, Electron Microscopy Sciences), known to be a non-polar resin. The resin was

polymerized under indirect UV light at 254 nm for 72h. Sections were made using an ultramicrotome (LEICA UC6). Cross-sections were placed on a ~1 cm^2 silicon wafer (Siltronix, France). Immunogold labeling of BMP-2 starts with two different blocking steps: first, the silicon wafer was immersed in a 50mM Glycine (G8898, Sigma) bath in PBS for 20 min and then blocked using 2% BSA (900.001, Aurion) in PBS for 1h. Mouse anti-BMP-2 (B9553, Sigma) at 2.5 µg/mL was used as a primary antibody and goat anti-mouse IgG conjugated to 10 nm gold NPs (G7652, Sigma) diluted 1:20 was used as secondary antibody. The sample was finally rinsed with milli-Q water and air dried for a few hours. For SEM imaging, the vCD backscatter detector of a Quanta 250 FEG (FEI Company) was used at a working distance of 7.3mm. The images were acquired at 5 keV and with a dwell time of 60 µs.

2.3 Cell culture and reagents

Murine C2C12 skeletal myoblasts (<15 passages, obtained from the American Type Culture Collection, ATCC) were cultured in tissue culture Petri dishes, in a 1:1 Dulbecco's Modified Eagle Medium (DMEM):Ham's F12 medium (Gibco, Invitrogen, France) supplemented with 10% fetal bovine serum (FBS, PAA Laboratories, France) and 100 U/mL penicillin G and 100 µg/mL streptomycin (Gibco, Invitrogen, France) in a 37 °C, 5% CO$_2$ incubator.

For BMP-2 internalization studies, 3×10^4cells/cm^2 were seeded on top of the films or on Thermanox® slides. After different contact times with bBMP-2 or sBMP-2 (5 min, 30 min, 1, 4, 8, 12, 24, 48 or 72 h), the cells were fixed with 3.7% formaldehyde in PBS for 20 min.

To evaluate the impact of endocytosis inhibitors on BMP-2 internalization, C2C12 cells were pre-incubated for 45 min with several chemical inhibitors of the endocytic pathways, including 20 µM of chlorpromazine (CPZ, Sigma), 200 µM of genistein (GST, Sigma), 25 µg/mL of nystatin (NYS, Sigma), 2 mM of methyl-β-cyclodextrin (MβCD, Sigma), or 40 µM of dynasore (DYN, Sigma). Pre-treated cells were seeded at 3×10^4 cells/cm^2 on top of the films or on Thermanox® slides and fixed after 8h of contact with bBMP-2 or sBMP-2.

2.4 Immunofluorescence staining

Fixed cells were permeabilized for 4 min in TBS (50 mM Tris-HCl, 0.15 M NaCl, pH 7.4) containing 0.2% Triton X-100. After rinsing with TBS, the cell samples were blocked for 1h at room temperature with 2% BSA (900.001, Aurion) in TBS. The samples were incubated for 1h at room temperature with the primary antibodies against BMP-2 (mouse anti-BMP-2, B9553Sigma, at 2.5 µg/mL), rab7 (rabbit anti-rab7, D95F2 Abcam, dilution 1:50), cav-1 (rabbit anti-cav-1, sc 894, Santa Cruz at 2 µg/mL), tubulin (mouse anti-β-tubulin, T4026, Sigma 1:200) and pSMAD1/5/8 (1:600, Cell Signaling). A 0.2% gelatin (G7765, Sigma) in TBS solution was used as incubation buffer. After extensive washing with TBS, the cells were further incubated with goat anti-mouse A647 (A21335, Invitrogen) or goat anti-rabbit A647 (A21244, Invitrogen) secondary antibodies diluted to 1:200 in 0.2% gelatin in TBS for 1h at room temperature. Actin was labeled with phalloidin-TRITC (1:800, Sigma) for 30 min. The cell nuclei were stained with 5 µg/mL of DAPI (Life Technologies) for 10 min. Nuclear p-SMAD1/5/8 intensity was measured over nucleus area, obtained from binarized nucleus images, using homemade Image J (National Institutes of Health) routines.

2.5 Transfection by siRNA

C2C12 cells were transfected with siRNA against BMP receptor Ia (BMPR-Ia), BMP receptor II (BMPR-II), clathrin heavy-chain (CHC), caveolin-1 (Cav-1) and dynamin-2 (DYN-2) (ON-TARGET plus SMARTpool, respectively Mouse BMPR-Ia, BMPR-II, Cltc, Cav1 and Dnm2 Thermo Scientific Dharmacon). A scrambled siRNA (all stars negative control siRNA, Qiagen) was taken as control. Cells were seeded at $3x10^4$ cells/cm^2 in 6-well plates and cultured in 2 mL of GM for 15h. The transfection protocol was followed as previously described [31]. After transfection the cells were detached by trypsin-EDTA, seeded in GM at $3x10^4$ cells/cm^2 on the films and allowed to adhere for 4h in the case of siRNA against receptors or 8h for siRNA against endocytic proteins.

2.6 Confocal microscopy observations

Confocal images were acquired with a Zeiss LSM 700 confocal laser scanning microscope (Zeiss, Le Peck, France) equipped with a 63x oil immersion objective and several laser diodes (405, 488, 555 and 639 nm). Fluorescence recovery after photobleaching (FRAP) experiments were conducted to evaluate BMP-2^{CF} diffusion inside the (PLL/HA) films. To this end, a 20 μm circular region of interest (ROI) was bleached using the 488 nm laser diode and the recovery after photobleaching was followed over time. The fluorescence intensity of the ROI was normalized to that of a control region.

2.7 Quantification of the internalized amounts of BMP-2

Images of the isolated cells taken with a 63x oil immersion objective were used to quantify the total BMP-2 vesicle area per cell. The quantification of the internalized BMP-2 by the cells over time and after different chemical treatments was performed using Image J software 1.44 (imagej.nih.gov/ij/). The total vesicle area per cell (in μm^2) in one confocal plane was quantified over the 0.02 - 5 μm^2 range after image thresholding using the "Analyze Particles" function. The experiments were repeated at least three times, with at least two samples per condition in each experiment, and 50 cells analyzed for each sample. For each experimental condition, the area of the internalized BMP-2 vesicle was fitted with an exponential function:

$$\text{Internalized BMP} - 2 = I_{max} * [1 - exp(-t/\tau)] \quad \text{Equation (1)}$$

Where τ is the characteristic time of BMP-2 internalization (in h), I_{max} is the plateau value (in *a.u.*)

2.8 Western blotting

Detection of proteins by Western blotting was done according to standard protocols. After electrotransfer and blocking (10 mM Tris, pH 7.9, 150 mM NaCl, 0.5% Tween 20, 3% dry milk at room temperature for 1 h), the PVDF membrane was incubated with primary antibodies overnight at 4°C, pSMAD1/5/8 (Cell Signaling), cav-1 (rabbit, Santa Cruz), clathrin heavy-chain (mouse, BD Biosciences) dynamin2 (goat, Santa Cruz). Immunological detection was achieved with a HRP-conjugated secondary antibody. Peroxidase activity was visualized by ECL (West pico signal, Pierce) using a ChemiDoc MP imaging system (Bio-

Rad). Densitometric quantification of the bands was performed using the Image Lab program (Bio-Rad). As a control, the detection of actin was also performed.

2.9 Alkaline Phosphatase (ALP) activity test

The impact of the siRNA-mediated knocking-down of endocytic proteins on non-canonical BMP-2 signaling pathway was determined by assaying the BMP-2-induced alkaline phosphatase (ALP) activity, a marker of osteogenic differentiation, following a previously established protocol [22]. First, the film was thoroughly washed with a Hepes-NaCl solution for at least 2h to discard any weakly bound or unbound BMP-2. Then, after transfection by siRNA, $9x10^4$ C2C12 cells were seeded on each film-coated glass slide in a 24-well plate. After 3 days of culture, the growth medium was removed and the cells were washed with PBS and lysed by sonication for 5s in 500μL of 0.1 % Triton-X100 in PBS. The ALP activity of these samples was then quantified using the standard protocol and normalized to the corresponding total protein content, which was determined using a bicinchoninic acid protein assay kit (Interchim, France). The same experiments were conducted for sBMP-2, for which a concentration of 600 ng/mL of BMP-2 was added to the medium.

2.10 Statistical analysis

Numerical results on the amount of internalized BMP-2 are mainly presented in box-and-whisker plots. In all other cases, they were reported as average ± standard error of the mean of several independent experiments. Data comparison was performed by *t-test* analysis test by comparing each experimental data group to the control one. Statistical analyses were conducted using SigmaPlot software. Statistically significant differences between the groups were identified in the images with * representing a *p* value < 0.01.

3 Results

3.1 BMP-2 trapping within (PLL/HA) films

For the purpose of BMP-2 loading in films, the film was initially loaded in a salt-free medium at pH 3, a pH at which BMP-2 is highly soluble [32]. At pH 3, protonation of HA in view of its polyelectrolyte character [33] can be clearly evidenced by infrared spectroscopy (Figure 1A). Such protonation may lead to film swelling and increased permeability to BMP-2. Increasing the pH to physiological levels using the Hepes-NaCl buffer at pH 7.4 reversibly decreases the protonation of HA (Figure 1B). The physiological conditions (pH 7.5 and presence of salt) being already known to be not favorable for BMP-2 solubility [32], BMP-2 can remain trapped in the film. A confocal view of a cross-section of the film where both BMP-2 (with BMP-2^{CF}) and film (labeled with Alexa 568) are labeled, which was performed several hours after extensive rinsing of the loaded films, effectively revealed that BMP-2 remained trapped in the polyelectrolyte film (Figure 2A). In our experimental conditions, the films made of 24 layer pairs have a typical thicknesses of the order of 5-6 μm. The corresponding fluorescence intensity profiles showed a partial BMP-2 vertical diffusion inside the film (Figure 2A, A'). This partial diffusion was also confirmed by immunogold labeling of BMP-2. On film cross-sections the gold nanoparticles are essentially visible in the upper part of the film (Figure 2B). The potential lateral diffusion of BMP-2 trapped in the films was analyzed by FRAP analysis (Figure 2C). No recovery of

fluorescence was observed several hours after photobleaching, indicating the absence of diffusion of bBMP-2 within the film once trapped in the film. This absence of diffusion correlates with the very low release of BMP-2 in the culture medium (< 10 ng/mL), once it has been thoroughly washed [22]. Finally, we also verified on film cross-sections imaged by SEM that the film remained intact after 24 h in the culture medium and in the presence of C2C12 cells (Figure 2D). Thus, the cells were still adhering on top of the films.

Altogether, our results showed that BMP-2 diffused inside the (PLL/HA) film during the loading phase at pH 3. After a thorough rinsing at physiological pH, BMP-2 was trapped in the polyelectrolyte film and therefore presented to the cells in a matrix-bound manner.

3.2 Differences between matrix-bound and soluble presentation of BMP-2

There are major differences between the bBMP-2 and sBMP-2 presentation modes (Figure 3). First, the lifetime for the bioactivity of bBMP-2 is at least several months in the case of bBMP-2 [25], in comparison to 13 h for sBMP-2 [34]. We have previously shown that these films are bioactive as they triggered short-term SMAD signaling [27] but also ALP after 3 days [22] and this even after over 6 months of storage [25]. Second, diffusion of bBMP-2 is restricted (Figure 2) while sBMP-2 is free to diffuse in a 3D volume [35]. In these conditions, bBMP-2 will interact with the cells by the ventral side while it will mostly interact with their dorsal side in the case of sBMP-2 [27]. Besides, it is known that cell adhesion defines the topology of endocytosis and signaling [36].

The sBMP-2 with cells on TCPS condition is the experimental condition used by biologists to study BMP-2-mediated signaling [29, 37] and can thus be considered as a "reference" condition. Indeed, it has already been shown, using radiolabeled BMP-2 or fluorescently labeled sBMP-2, that sBMP-2 is internalized by cells [37–39]. For this reason, we decided to also study sBMP-2 as a "positive" control and to include both films and TCPS as underlying substrate materials. Interestingly, the comparison of sBMP-2 delivered from a biomaterial of controlled crosslinking or from TPCS will enable us to reveal whether there is a biomaterial-dependent internalization of sBMP-2.

3.3 Matrix-bound BMP-2 can be internalized by C2C12 myoblasts

We used BMP-2^{CF} to investigate the internalization of bBMP-2 by C2C12 cells (Figure 4), since we previously proved that the bioactivity of BMP-2^{CF} is similar to that of unlabeled BMP-2 [22]. As C2C12 cells typically need 4h to adhere and spread on bBMP-2 [27], it is likely that cell spreading on films and bBMP-2 internalization will occur simultaneously. Indeed, we first observed that bBMP-2^{CF} was internalized in the form of endocytic vesicles (Figure 4A), whose number and size increased as a function of time. After 4h in contact with the films loaded with BMP-2^{CF}, several BMP-2^{CF} vesicles can be observed inside adherent cells (Figure 4A and B), at the cell/film interface but also above the nucleus (Figure 4C). Anti-BMP-2 immunolabeling of C2C12 cells spread onto a (PLL/HA) film loaded with BMP-2^{CF} film demonstrated the double staining of vesicles, confirming the presence of BMP-2^{CF} inside the fluorescent vesicles (Figure 4D). As a control, the specificity of the BMP-2 uptake by C2C12 cells was confirmed by testing their inability to internalize BSA-

FITC loaded in the films. (Figure SI1). Thus, BMP-2^{CF} trapped in the film can be specifically internalized by C2C12 cells.

3.4 Internalization of matrix-bound BMP-2 is controlled by the level of film crosslinking

We then studied the influence of film crosslinking on the internalization kinetics of bBMP-2 in comparison to that of sBMP-2. Representative images of a cell at the endpoint of the experiment (3 days) in contact with bBMP-2 delivered from the differently crosslinked films (EDC10, 30 and 70) are shown in Figure 5A. The quantity of internalized BMP-2- decreased with the degree of film crosslinking, as confirmed by the quantitative analysis over time of the amount of internalized bBMP-2 per cell (Figure 5B, Table 1). Indeed, internalization was significantly higher for EDC10 films, reaching a plateau value I_{max} of 21.5 ± 0.6 μm^2/cell, as compared to $\sim 8.7 \pm 1.5$ μm^2/cell and 2.9 ± 0.8 μm^2/cell for EDC30 and 70 respectively, after 3 days. This represents a 7-fold higher amount of internalized bBMP-2 for EDC10 in comparison to EDC70. In contrast with bBMP-2, sBMP-2 was equally internalized by cells cultured on films (EDC10 and 70) or on Thermanox® slides (Figure 5C and Table 1), at 11 $\sim$ μm^2/cell, but the absolute amounts were systematically lower than for the bMBP-2 counterparts.

However, a direct comparison between the Imax in the case of sBMP-2and bBMP-2 cannot be made. It is already known that BMP-2 has a short lifetime of ~13 h in solution [34]. For sBMP-2, the reservoir of accessible BMP-2 is lower in amount and is also limited in time. In contrast, in the case of bBMP-2, the film acts as a nano-reservoir that can continuously provide bBMP-2 to cells "on demand". Secondly, the delivery mode is fundamentally different (Figure 3B): internalization of soluble molecules, as is the case here for sBMP-2, is essentially mediated at the *dorsal* side of the cell [36] while bBMP-2 internalization is *solely* mediated at the *ventral* side of the cell, due to the spatial confinement of bBMP-2.

For this reason, we plotted the same data in a different way after normalization of each kinetic curve by its corresponding plateau value (i.e. the *Imax* values of Table 1) (Figure 5D and E). This enables us to directly compare the conditions independently of their plateau value and to focus *solely* on the kinetics aspect, since the internalized amounts are so different and do not allow us to capture the internalization kinetics. At first sight, it appears that internalization was the fastest when there was no film, i.e. for the TCPS condition ($\tau \sim$ 2-3 h). Interestingly, the internalization kinetics parameters (τ) were similar for bBMP-2 and sBMP-2 on EDC10, but internalization was much faster (i.e. lower τ) for sBMP-2 on TCPS and EDC70 films in comparison to bBMP-2 (Figure 5D, E and Table 1). In addition, for bBMP-2, τ also depended on the EDC concentration and was in the order EDC10 < EDC30 < EDC70 (Table 1), which indicates that internalization is facilitated on the lowest crosslinked films (EDC10).

Importantly, the increased internalization and kinetics of BMP-2 internalization for cells on EDC10 cannot be attributed to an increased amount of BMP-2 in these films, as these films retained the lowest amount of BMP-2 in comparison to the more crosslinked films (Table SI1). We also noted that, when pooling all data together, no direct relationship between the cell spreading area and the amount of internalized BMP-2 was evidenced (Figure SI2). In addition, the analysis of the size of BMP-2 vesicles at 8 h (Figure SI3) revealed that, for

EDC10 and EDC30 conditions, 80 % of the vesicles were below 0.5 μm^2 and the remaining fraction above; for the more crosslinked EDC70 films, there was a single population -95%- of very small vesicles (below 0.5 μm^2).

All together, these data showed that internalization of bBMP-2 was greatly facilitated (higher amount and faster kinetics) on the low crosslinked EDC10 films. In contrast, the internalization kinetics were mostly independent of the underlying matrix in the case of sBMP-2.

3.5 BMPR-Ia and BMPR-II are involved in BMP-2 uptake by C2C12 cells

Although it has been shown that BMP receptors are internalized following activation [9], little is known about the ability of their ligand (i.e. BMP-2), to be internalized. In the following experiments, we focused on the internalization of bBMP-2 on EDC10 films, for which the highest amount of internalized BMP-2 was observed. To address whether specific BMP receptors may be involved in BMP2^{CF} ligand uptake, C2C12 cells were treated or not with siRNA directed against BMPRIa and BMPRII before spreading onto BMP-2-loaded films. (Figure 6). Comparing BMP-2^{CF} ligand internalization in WT and siRNA-treated C2C12 cells, a clear decrease of the BMP-2 uptake upon deletion of BMPRIa or BMPR-II was observed (Figure 6A) (Figure 5B). Knockdown of BMPR-Ia and of BMPR-II significantly decreased the amount of internalized BMP-2 to respectively ~ 50% and ~ 38 % of the control values (Figure 6C). The efficacy of the siRNA against BMPR-Ia and BMPR-II receptors was confirmed by quantitative PCR (Figure 6C).

These results show that both BMPR-Ia and BMPR-II are critical for mediating the internalization of matrix-bound BMP-2.

3.6 Caveolin, clathrin and dynamin are involved in the internalization of matrix-bound BMP-2

In conditions where BMP-2 is presented to the cells in a soluble form, it has been suggested that BMPRs are internalized by two distinct mechanisms which are based on either clathrin- or caveolin-mediated processes [29, 40] and associated with specific BMP signaling pathways [29]. Using a pharmacological approach and a siRNA strategy against different endocytic pathways, we explored which of these mechanisms mediated the observed matrix-bound BMP-2 ligand internalization as compared to sBMP2 (Figure 7). First, we observed some colocalization of BMP-2^{CF} vesicles and caveolin-1 (Figure 7A), a marker for caveolae internalization [41–43], as well as with rab7 (Figure 7A), a later marker for clathrin-dependent internalization [43, 44].Then, we investigated the impact of inhibitors of clathrin- and caveolae-dependent endocytosis. Chlorpromazine (CPZ) is known to disturb clathrin-dependent endocytosis [45], genistein (GST) and nystatin (NYS) perturb lipid rafts/caveolin-dependent endocytosis [46, 47]. Methyl-β-cyclodextrin (MβCD) interferes with lipid rafts and has also been shown to inhibit clathrin-dependent endocytosis [48]. Finally, we studied the effect of dynasore (DYN), known to affect both clathrin and lipid rafts/caveolin-dependent endocytosis by blocking the GTPase activity of dynamin [49], thus impeding the scission of newly-formed vesicles from the membrane. When BMP-2 was presented as bBMP-2 (Figure 7B) or sBMP-2 (Figure SI5), no effect was observed after treatment with

CPZ. In contrast, a significant decrease of up to 50-60% in the internalization was observed after treatment with GST, NYS or MβCD. DYN had the strongest effect and blocked ~70% of BMP-2 internalization (Figure 7B and SI5). To note, the results obtained for bBMP-2 (Figure 7) and sBMP-2 (Figure SI5A) were qualitatively similar.

The specific effects of clathrin, caveolin and dynamin on bBMP-2^{CF} endocytosis were quantified after siRNA treatments (Figure 6C), which were validated by Western blotting (Figure 6D). For the inhibition, the isoform 2 of dynamin (DYN-2) was selected in view of its major importance in muscle [50]. Again, similar results were obtained for bBMP-2 and sBMP-2 (Figures SI5B), with a decrease of ~70% of the internalized amount when CHC, CAV-1or DYN-2 were knocked-down. The effects of the siRNA knockdown of endocytic proteins were systematically stronger than those of the pharmacological inhibitors.

Altogether, these results indicate that both clathrin- and caveolin-dependent endocytosis are involved in the bBMP-2^{CF} uptake and that the internalization pathways for bBMP-2 are similar to those of sBMP-2.

3.7 Endocytosis route of bBMP-2 is related to signaling

Endocytosis and signal transduction are intertwined processes [51–53]. Whereas clathrin-dependent BMP receptor internalization has been shown to be involved in canonical SMAD signaling [29], caveolin-dependent mechanisms have been described as associated with either non-canonical [29] or canonical signaling [54]. To date, little is known on the relation between the internalization of the BMP-2 ligand and BMP signaling.

We studied the effect of endocytic pathway inhibition by the siRNA-mediated knockdown strategy on BMP-2 signaling pathways in conditions where BMP-2 is presented by the biomaterial (Figure 8) in comparison to sBMP-2 (Figure SI6). The nuclear localization (Figure 8A,B) and phosphorylation of SMAD1/5/8 (Figure 8C) were taken as hallmarks of SMAD-dependent signaling while ALP activity (Figure 8D) was representative of the non-canonical mitogen activated protein kinase (MAPK) pathway [11] [9]. Indeed, ALP expression was shown to be dependent on the p38 MAPK pathway activation in vitro in osteoblasts [55] and C2C12 cells [56] and in vivo in mice [57]. The knockdown of CAV-1 significantly decreased the nuclear localization of pSMAD (Figure 8A, B) as compared to siControl or siCHC. In contrast, knockdown of DYN-2 even increased the nuclear localization of pSMAD. These different effects were correlated with the phosphorylation of SMAD analyzed by western blot (Figure 8C, SI6). Indeed, deletion of CAV-1 drastically decreased the amount of pSMAD in comparison to the deletion of CHC or DYN-2, this latter giving similar results to the control value. In contrast, knockdown of both CAV-1 and CHC strongly decreased ALP expression (Figure 8D) while it was insensitive to the knockdown of DYN-2. Similar results were obtained for sBMP-2 for SMAD nuclear localization, phosphorylation and for ALP activity (Figure SI6).

Altogether, these results show that SMAD signaling is essentially dependent on caveolin whereas the ALP pathway depends on both caveolin and clathrin heavy chain. In contrast, DYN-2 was fully dispensable for the phosphorylation of SMAD, its translocation to the nucleus and for ALP signaling.

3.8 ALP activity depends on the level of film crosslinking but not the phosphorylation of SMAD

Finally, we studied whether the phosphorylation of SMAD and ALP could be related to the level of film crosslinking (Figure 9). In our experimental conditions (films made of 24 layer pairs and loaded with BMP-2 at 20 mg/mL), pSMAD appears to be independent on the crosslinking level of the film (Figure 9A). In contrast, the ALP activity is the highest for the low crosslinked films (EDC10) and significantly decreases when EDC increases (ie when the film stiffness increases) (Figure 9B). To note, the negative controls (absence of BMP-2) confirm that there is a negligeable pSMAD signal (Figure 9A) and absolutely no ALP signal (Figure 9B) in the absence of BMP-2. The pSMAD and ALP signals for TCPS in the presence of sBMP-2 were similar to those of EDC70 films.

This result proves that, while pSMAD is independent of film stiffness, ALP is inversely correlated with the film stiffness, with a higher signal for the lowest film stiffness.

Finally, we summarize our finding regarding the clathrin and caveolin-1 signaling by a new schematic (Figure 9C) : while both CHC and Cav-1 contribute to the ALP signal, only Cav-1 impacts pSMAD signaling.

4 Discussion

A close insight into the diffusion of bioactive molecules within a biomaterial carrier and their ability to be internalized is essential to better understand the coupling between the endocytosis of bioactive molecules and signaling for cell commitment and tissue regeneration. Here, we explored the process of BMP-2 trapping in a biopolymeric thin film, its delivery and endocytosis-dependent BMP-2 signaling. First we have shown that the degree of crosslinking controls BMP-2 endocytosis (Figure 5), highlighting the fact that bBMP-2 internalization depends on film stiffness. Film crosslinking can thus be used to optimize endocytosis of matrix-bound BMP-2 by cells. Secondly we showed that endocytosis of bBMP-2 is continuous but slower in comparison to sBMP-2 (Table 1), which can be explained by the restricted diffusion of bBMP-2 in comparison to freely diffusing BMP-2, and also by the fact that cells first need to spread on the film before being able to internalize bBMP-2 by their ventral side. Thirdly our results demonstrate a tight coupling between BMP-2 internalization and signaling: i) endocytosis via caveolin can lead to both SMAD and ALP pathways; ii) endocytosis via clathrin triggers only ALP; iii) The early steps of internalization implying protein recruitment to the endocytic sites are more important than the subsequent vesicle scission, since the silencing of Dyn2 did not alter signaling.

4.1 C2C12 as a simple cellular model of BMP-2-responsive cells to study the early steps of BMP-2-mediated bone formation

Why did we choose C2C12 myoblasts as a simple cellular model for this bBMP-2-mediated cell internalization study? First, although C2C12 are skeletal myoblasts, there is abundant literature on BMP and C2C12 myoblasts in the bone field, simply because these cells are a very robust, reliable, and easy to implant model system to study BMP-2 signaling [5, 58]

and also because the role of BMP-2 in muscle biology is progressively beginning to be unraveled [59]. C2C12 cells are mesenchymal precursors [60, 61]. The BMP receptor repertoire is cell type specific and has already been well studied for C2C12 [62]. In 1994, Katagiri et al. showed for the first time that soluble BMP-2 in solution can trigger a *specific* response in C2C12 cells, which is BMP-2 dose dependent [5]. Advantageously, the ALP response of C2C12 cells to sBMP-2 is very clear with an "off/on" switch that is specifically due to the presence of sBMP-2. This is in contrast to osteoblastic precursors, such as MC3T3-E1 or mesenchymal stem cells, who always express a basal and non-negligible level of ALP [34]. C2C12 cell response to BMP-2 is fast, with ALP and osterix (a bone marker) being typically measured after 3 days, while it is late for stem cells (it needs at least one or two weeks to be quantitatively measured for stem cells [17]). For bBMP-2, our group has already proved that C2C12 cells respond to matrix-bound BMP-2 presented from polyelectrolyte films and that the cell response is BMP-2 dose-dependent [22]. In our latest studies, we have shown that the adsorbed amount of BMP-2 can be tuned depending on the crosslinking level of the film (EDC10, EDC30, EDC70) (see Table SI1 taken from [25]) and that C2C12 cells respond to these different amounts by expressing ALP and activating SMAD signaling [27, 28].

4.2 The physical properties of the biomaterial control internalization of matrix-bound BMP-2

Our results show for the first time that BMP-2 presented by a carrier biomaterial, such as (PLL/HA) polyelectrolyte films, is internalized by the cells with a characteristic time scale τ between 7 and 40 h (Figure 5, Table 1). A continuous increase of the amount of internalized vesicles was observed with no decrease over at least 3 days, likely resulting from the reservoir nature of the biomimetic film, the non-diffusive property of BMP-2 once trapped in the film (Figure 3) and the fact that cells can internalize bBMP-2 by their ventral side (Figure 3 and 4). Our data for bBMP-2 are thus consistent with previous data on sBMP-2 showing a continuous increase in the amount of BMP-2 internalized over 3 days [39]. Internalization of sBMP-2 was faster, which can be attributed to the free diffusion of sBMP-2 in the cell culture medium and ease of cellular internalization by the dorsal side of the cells.

We found that the physical properties of the (PLL/HA) film, and in particular the crosslinking (stiffness) of the film was key in endocytosis since i) the uptake of bBMP-2 was the highest (Figure 5A) and fastest on the low crosslinked (softest) films, with a 7-fold increase in the internalized amount and 5-fold increase in kinetics in comparison to the stiff film (EDC70); ii) the differences between the uptake of bBMP-2 and sBMP-2, for a given underlying matrix, depended on substrate stiffness (Figure 5 D,E). To sum up, cells on soft films with bBMP-2 were able to rapidly internalize a very high amount of bBMP-2, similarly to sBMP-2 (Figure 5D), while cells on the stiff films with bBMP-2 exhibited a strongly impaired internalization in comparison to sBMP-2 (Figure 5E), with very small internalization vesicles (Figure SI3).

It is worth noting that this stiffness-sensitive endocytosis cannot be attributed to a difference in the available amount of bBMP-2 since, precisely, this amount was lowest on EDC10 films

(Table S1). Interestingly, our results are in line with previous studies showing an increase of BMPR internalization on a soft substrate [42].

4.2 BMP receptors, clathrin and caveolin pathways are involved in matrix-bound BMP-2 internalization

Whether and how the endocytosis mechanism is related to BMP-2 signaling is a key question for biomaterial optimization and control of cell commitment. Using the siRNA-mediated knockdown of BMPR-Ia and BMPR-II receptors, we showed that both receptors are involved in the BMP-2 internalization process (Figure 6). These results are consistent with those of other studies showing the importance of BMPR in BMP protein internalization [37, 43]. Indeed, Alborzinia *et al.* observed an increase in the amount of BMP-2 internalized after overexpression of BMPR-Ia [37]. Kelley *et al.* also showed that internalization of BMP-4 decreased for cells expressing a mutant BMPR-II with no cytoplasmic extension downstream of the kinase domain [43].

It is known that BMPR-Ia and BMPR-II receptors can be internalized via different endocytic pathways, especially caveolae and clathrin-coated pits [29, 40, 63]. Using complementary experimental approaches with inhibitors of endocytosis and an siRNA strategy targeting endocytic pathways, we showed that bBMP-2, similarly to sBMP-2 (Figure 6 and Figure SI6), is internalized through both caveolin and clathrin-dependent pathways, although with some quantitative differences. Our results are globally in agreement with previous studies using chemical inhibitors such as DYN, CPZ, GST and NYS, [39, 58, 64], showing that sBMP-2 was internalized through caveolin- and clathrin-dependent pathways in C2C12 cells. However, in contrast to previous studies [37, 39], we did not observe any effect of CPZ. This may be due either to the strong and peculiar effect of this drug on the shape of endocytic vesicles (Figure SI4), or to an alternative internalization route taken in the presence of this drug, or even by the difference in cell type (C2C12 cells versus Hela cells [37]).

4.3 Endocytocis of matrix-bound BMP-2 is related to BMP-2 signaling

Altogether, our results for bBMP-2 or those obtained for sBMP-2 (Figure 8 and Figure S6) show that (i) caveolin mediates both SMAD and non-SMAD signaling (ii) clathrin mediates only ALP signaling and (iii) the scission via dynamin and subsequent transport of caveolae and clathrin vesicles is not required for neither SMAD nor ALP signaling. It is known that the knockdown of dynamin blocks the scission and pinch-off of the vesicles from the plasma membrane, thus affecting intracellular trafficking [65, 66]. Therefore, our results show that, even in the absence of BMP-2 internalization (Figure 7) and vesicle scission (Figure 8), signaling can still occur at the plasma membrane. This result fully agrees with a recently published manuscript highlighting that dynamin-2 is dispensable for BMP-2 signaling [67].

Our results are consistent with the previous studies on the role of CAV-1 in mediating SMAD signaling by sBMP-2 [54], and on the important role of BMPR-IA in this process [40]. It may well be that the knockdown of CAV-1 and CHC perturbs the clustering of BMP-2/BMP receptors, ultimately impeding the activation of signaling pathways.

Interestingly, our results are consistent with very recent findings showing that i) pSMAD can be triggered in a ligand-independent manner by inducing the clustering of BMP receptors via immunoglobulins [68] and ii) BMP-2 covalently crosslinked to gold nanoparticles is able to induce SMAD signaling without BMP-2 internalization [69]. In sum, internalization is not necessary for SMAD or ALP signaling.

Our results on C2C12 myoblasts and polyelectrolyte films how that the physico-chemical properties, film crosslinking, in other words film stiffness, can affect BMP-2 trafficking. Our results on C2C12 myoblasts are consistent with recent studies on cells, including but not limited to muscle cells, which showed the key role of Cav-1 as a physiological reservoir of lipids that can accommodate sudden and acute mechanical stresses [61]. We can anticipate that a softer environment (i.e. film EDC10) is correlated to a lower tension of the cell membrane, which is able to control the shape of the clathrin or caveolin coat, as already described [70]. Indeed, high tension of the membrane of model cells (giant vesicles) has recently been shown to hinder the closure of clathrin-coated pits [71]. The role of Cav-1 in the "mechano-protection" of the cell lipid membrane by preventing mechanical damage in response to an increased membrane tension [60] has only recently begun to be unraveled [59]. Our results open avenues for future mechanistic studies aimed at better understanding the underlying molecular mechanisms and their relation to the formation of regenerated bone.

Conclusions

Our results show for the first time that cells can internalize matrix-bound BMP-2 presented from a biomaterial. We demonstrated that the presence of caveolin-1 at the plasma membrane is required for SMAD and ALP signaling, while the presence of clathrin at the membrane is only required for ALP signaling. Signaling can be triggered at the plasma membrane without the need for the Cav-1 and clathrin vesicles to be pinched-off. However, in contrast to soluble BMP-2, the internalization of matrix-bound BMP-2 depends on the physical properties of the underlying matrix: both the internalized amount, the internalization kinetics and ALP activity strongly depend on the level of film crosslinking. The optimization of BMP-2 endocytosis and signaling via engineered biomaterials will open new and innovative strategies for improved bone regeneration therapies.

Supplementary Material

Refer to Web version on PubMed Central for supplementary material.

Acknowledgements

Bibliographic references

[1]. Urist MR. Bone: formation by autoinduction. Science. 1965; 150:893–9. [PubMed: 5319761]

[2]. Hogan BL. Bone morphogenetic proteins: multifunctional regulators of vertebrate development. Genes Dev. 1996; 10:1580–94. [PubMed: 8682290]

[3]. Simic P, Vukicevic S. Bone morphogenetic proteins: from developmental signals to tissue regeneration. Conference on bone morphogenetic proteins. EMBO Rep. 2007; 8:327–31. [PubMed: 17363970]

[4]. Asakura A, Komaki M, Rudnicki M. Muscle satellite cells are multipotential stem cells that exhibit myogenic, osteogenic, and adipogenic differentiation. Differentiation. 2001; 68:245–53. [PubMed: 11776477]

[5]. Katagiri T, Yamaguchi A, Komaki M, Abe E, Takahashi N, Ikeda T, Rosen V, Wozney JM, Fujisawa-Sehara A, Suda T. Bone morphogenetic protein-2 converts the differentiation pathway of C2C12 myoblasts into the osteoblast lineage. J Cell Biol. 1994; 127:1755–66. [PubMed: 7798324]

[6]. Rickard DJ, Sullivan TA, Shenker BJ, Leboy PS, Kazhdan I. Induction of rapid osteoblast differentiation in rat bone marrow stromal cell cultures by dexamethasone and BMP-2. Dev Biol. 1994; 161:218–28. [PubMed: 8293874]

[7]. Nickel J, Sebald W, Groppe JC, Mueller TD. Intricacies of BMP receptor assembly. Cytokine Growth Factor Rev. 2009; 20:367–77. [PubMed: 19926516]

[8]. Mueller TD, Nickel J. Promiscuity and specificity in BMP receptor activation. FEBS Lett. 2012; 586:1846–59. [PubMed: 22710174]

[9]. Sieber C, Kopf J, Hiepen C, Knaus P. Recent advances in BMP receptor signaling. Cytokine Growth Factor Rev. 2009; 20:343–55. [PubMed: 19897402]

[10]. Wang RN, Green J, Wang Z, Deng Y, Qiao M, Peabody M, Zhang Q, Ye J, Yan Z, Denduluri S, Idowu O, et al. Bone Morphogenetic Protein (BMP) signaling in development and human diseases. Genes Dis. 2014; 1:87–105. [PubMed: 25401122]

[11]. Nohe A, Hassel S, Ehrlich M, Neubauer F, Sebald W, Henis YI, Knaus P. The mode of bone morphogenetic protein (BMP) receptor oligomerization determines different BMP-2 signaling pathways. J Biol Chem. 2002; 277:5330–8. [PubMed: 11714695]

[12]. Schmidmaier G, Schwabe P, Strobel C, Wildemann B. Carrier systems and application of growth factors in orthopaedics. Injury. 2008; 39(Suppl 2):S37–43.

[13]. Carragee EJ, Hurwitz EL, Weiner BK. A critical review of recombinant human bone morphogenetic protein-2 trials in spinal surgery: emerging safety concerns and lessons learned. Spine J. 2011; 11:471–91. [PubMed: 21729796]

[14]. Reddi AH, Reddi A. Bone morphogenetic proteins (BMPs): from morphogens to metabologens. Cytokine Growth Factor Rev. 2009; 20:341–2. [PubMed: 19900831]

[15]. Belair DG, Le NN, Murphy WL. Design of growth factor sequestering biomaterials. Chem Commun (Camb). 2014; 50:15651–68. [PubMed: 25182455]

[16]. Martino MM, Briquez PS, Guc E, Tortelli F, Kilarski WW, Metzger S, Rice JJ, Kuhn GA, Muller R, Swartz MA, Hubbell JA. Growth factors engineered for super-affinity to the extracellular matrix enhance tissue healing. Science. 2014; 343:885–8. [PubMed: 24558160]

[17]. Phillippi JA, Miller E, Weiss L, Huard J, Waggoner A, Campbell P. Microenvironments engineered by inkjet bioprinting spatially direct adult stem cells toward muscle- and bone-like subpopulations. Stem Cells. 2008; 26:127–34. [PubMed: 17901398]

[18]. Boerckel JD, Kolambkar YM, Dupont KM, Uhrig BA, Phelps EA, Stevens HY, Garcia AJ, Guldberg RE. Effects of protein dose and delivery system on BMP-mediated bone regeneration. Biomaterials. 2011; 32:5241–51. [PubMed: 21507479]

[19]. Shekaran A, Garcia JR, Clark AY, Kavanaugh TE, Lin AS, Guldberg RE, Garcia AJ. Bone regeneration using an alpha 2 beta 1 integrin-specific hydrogel as a BMP-2 delivery vehicle. Biomaterials. 2014; 35:5453–61. [PubMed: 24726536]

[20]. Kisiel M, Ventura M, Oommen OP, George A, Walboomers XF, Hilborn J, Varghese OP. Critical assessment of rhBMP-2 mediated bone induction: an in vitro and in vivo evaluation. J Control Release. 2012; 162:646–53. [PubMed: 22902595]

[21]. Patterson J, Siew R, Herring SW, Lin AS, Guldberg R, Stayton PS. Hyaluronic acid hydrogels with controlled degradation properties for oriented bone regeneration. Biomaterials. 2010; 31:6772–81. [PubMed: 20573393]

[22]. Crouzier T, Ren K, Nicolas C, Roy C, Picart C. Layer-by-Layer films as a biomimetic reservoir for rhBMP-2 delivery: controlled differentiation of myoblasts to osteoblasts. Small. 2009; 5:598–608. [PubMed: 19219837]

[23]. Dierich A, Le Guen E, Messaddeq N, Stoltz S, Netter P, Schaaf P, Voegel J-C, Benkirane-Jessel N. Bone formation mediated by synergy-acting growth factors embedded in a polyelectrolyte multilayer film. Adv Mater. 2007; 19:693–7.

[24]. Crouzier T, Sailhan F, Becquart P, Guillot R, Logeart-Avramoglou D, Picart C. The performance of BMP-2 loaded TCP/HAP porous ceramics with a polyelectrolyte multilayer film coating. Biomaterials. 2011; 32:7543–54. [PubMed: 21783243]

[25]. Guillot R, Gilde F, Becquart P, Sailhan F, Lapeyrere A, Logeart-Avramoglou D, Picart C. The stability of BMP loaded polyelectrolyte multilayer coatings on titanium. Biomaterials. 2013; 34:5737–46. [PubMed: 23642539]

[26]. Gilde F, Maniti O, Guillot R, Mano JF, Logeart-Avramoglou D, Sailhan F, Picart C. Secondary structure of rhBMP-2 in a protective biopolymeric carrier material. Biomacromolecules. 2012; 13:3620–6. [PubMed: 22967015]

[27]. Crouzier T, Fourel L, Boudou T, Albiges-Rizo C, Picart C. Presentation of BMP-2 from a soft biopolymeric film unveils its activity on cell adhesion and migration. Adv Mater. 2011; 23:H111–8. [PubMed: 21433098]

[28]. Fourel L, Valat A, Faurobert E, Guillot R, Bourrin-Reynard I, Ren K, Lafanechere L, Planus E, Picart C, Albiges-Rizo C. beta3 integrin-mediated spreading induced by matrix-bound BMP-2 controls Smad signaling in a stiffness-independent manner. J Cell Biol. 2016; 212:693–706. [PubMed: 26953352]

[29]. Hartung A, Bitton-Worms K, Rechtman MM, Wenzel V, Boergermann JH, Hassel S, Henis YI, Knaus P. Different routes of bone morphogenic protein (BMP) receptor endocytosis influence BMP signaling. Mol Cell Biol. 2006; 26:7791–805. [PubMed: 16923969]

[30]. Dingal PC, Discher DE. Combining insoluble and soluble factors to steer stem cell fate. Nat Mater. 2014; 13:532–7. [PubMed: 24845982]

[31]. Gribova V, Gauthier-Rouviere C, Albiges-Rizo C, Auzely-Velty R, Picart C. Effect of RGD functionalization and stiffness modulation of polyelectrolyte multilayer films on muscle cell differentiation. Acta Biomater. 2013; 9:6468–80. [PubMed: 23261924]

[32]. Abbatiello SE, Porter TJ. Anion-mediated precipitation of human recombinant protein 2 (Rh-BMP2) is dependent upon the heparin binding N-terminal region. Protein Science. 1997:99. poster presentation, Protein Society Meeting Boston. [PubMed: 9007981]

[33]. Haxaire K, Marechal Y, Milas M, Rinaudo M. Hydration of hyaluronan polysaccharide observed by IR spectrometry. II. Definition and quantitative analysis of elementary hydration spectra and water uptake. Biopolymers. 2003; 72:149–61. [PubMed: 12722111]

[34]. Takada T, Katagiri T, Ifuku M, Morimura N, Kobayashi M, Hasegawa K, Ogamo A, Kamijo R. Sulfated polysaccharides enhance the biological activities of bone morphogenetic proteins. J Biol Chem. 2003; 278:43229–35. [PubMed: 12912996]

[35]. Cantor, CR.; Schimmel, PR. Biophysical Chemistry. Oxford, England: Freeman; 1998.

[36]. Grossier JP, Xouri G, Goud B, Schauer K. Cell adhesion defines the topology of endocytosis and signaling. EMBO J. 2014; 33:35–45. [PubMed: 24366944]

[37]. Alborzinia H, Schmidt-Glenewinkel H, Ilkavets I, Breitkopf-Heinlein K, Cheng X, Hortschansky P, Dooley S, Wolfl S. Quantitative kinetics analysis of BMP2 uptake into cells and its modulation by BMP antagonists. J Cell Sci. 2013; 126:117–27. [PubMed: 23077176]

[38]. Jortikka L, Laitinen M, Lindholm TS, Marttinen A. Internalization and intracellular processing of bone morphogenetic protein (BMP) in rat skeletal muscle myoblasts (L6). Cell Signal. 1997; 9:47–51. [PubMed: 9067629]

[39]. von Einem S, Erler S, Bigl K, Frerich B, Schwarz E. The pro-form of BMP-2 exhibits a delayed and reduced activity when compared to mature BMP-2. Growth Factors. 2011; 29:63–71. [PubMed: 21391795]

[40]. Bragdon B, D'Angelo A, Gurski L, Bonor J, Schultz KL, Beamer WG, Rosen CJ, Nohe A. Altered plasma membrane dynamics of bone morphogenetic protein receptor type Ia in a low bone mass mouse model. Bone. 2012; 50:189–99. [PubMed: 22036911]

[41]. Di Guglielmo GM, Le Roy C, Goodfellow AF, Wrana JL. Distinct endocytic pathways regulate TGF-beta receptor signalling and turnover. Nat Cell Biol. 2003; 5:410–21. [PubMed: 12717440]

[42]. Du J, Chen X, Liang X, Zhang G, Xu J, He L, Zhan Q, Feng XQ, Chien S, Yang C. Integrin activation and internalization on soft ECM as a mechanism of induction of stem cell differentiation by ECM elasticity. Proc Natl Acad Sci U S A. 2011; 108:9466–71. [PubMed: 21593411]

[43]. Kelley R, Ren R, Pi X, Wu Y, Moreno I, Willis M, Moser M, Ross M, Podkowa M, Attisano L, Patterson C. A concentration-dependent endocytic trap and sink mechanism converts Bmper from an activator to an inhibitor of Bmp signaling. J Cell Biol. 2009; 184:597–609. [PubMed: 19221194]

[44]. Bucci C, Thomsen P, Nicoziani P, McCarthy J, van Deurs B. Rab7: a key to lysosome biogenesis. Mol Biol Cell. 2000; 11:467–80. [PubMed: 10679007]

[45]. Wang LH, Rothberg KG, Anderson RG. Mis-assembly of clathrin lattices on endosomes reveals a regulatory switch for coated pit formation. J Cell Biol. 1993; 123:1107–17. [PubMed: 8245121]

[46]. Aoki T, Nomura R, Fujimoto T. Tyrosine phosphorylation of caveolin-1 in the endothelium. Exp Cell Res. 1999; 253:629–36. [PubMed: 10585286]

[47]. Rothberg KG, Heuser JE, Donzell WC, Ying YS, Glenney JR, Anderson RG. Caveolin, a protein component of caveolae membrane coats. Cell. 1992; 68:673–82. [PubMed: 1739974]

[48]. Rodal SK, Skretting G, Garred O, Vilhardt F, van Deurs B, Sandvig K. Extraction of cholesterol with methyl-beta-cyclodextrin perturbs formation of clathrin-coated endocytic vesicles. Mol Biol Cell. 1999; 10:961–74. [PubMed: 10198050]

[49]. Macia E, Ehrlich M, Massol R, Boucrot E, Brunner C, Kirchhausen T. Dynasore, a cell-permeable inhibitor of dynamin. Dev Cell. 2006; 10:839–50. [PubMed: 16740485]

[50]. Leikina E, Melikov K, Sanyal S, Verma SK, Eun B, Gebert C, Pfeifer K, Lizunov VA, Kozlov MM, Chernomordik LV. Extracellular annexins and dynamin are important for sequential steps in myoblast fusion. J Cell Biol. 2013; 200:109–23. [PubMed: 23277424]

[51]. Chen YG. Endocytic regulation of TGF-beta signaling. Cell Res. 2009; 19:58–70. [PubMed: 19050695]

[52]. Sorkin A, von Zastrow M. Endocytosis and signalling: intertwining molecular networks. Nat Rev Mol Cell Biol. 2009; 10:609–22. [PubMed: 19696798]

[53]. Gonnord P, Blouin CM, Lamaze C. Membrane trafficking and signaling: two sides of the same coin. Semin Cell Dev Biol. 2012; 23:154–64. [PubMed: 22085846]

[54]. Saldanha S, Bragdon B, Moseychuk O, Bonor J, Dhurjati P, Nohe A. Caveolae regulate Smad signaling as verified by novel imaging and system biology approaches. J Cell Physiol. 2013; 228:1060–9. [PubMed: 23041979]

[55]. Suzuki A, Guicheux J, Palmer G, Miura Y, Oiso Y, Bonjour JP, Caverzasio J. Evidence for a role of p38 MAP kinase in expression of alkaline phosphatase during osteoblastic cell differentiation. Bone. 2002; 30:91–8. [PubMed: 11792570]

[56]. Gallea S, Lallemand F, Atfi A, Rawadi G, Ramez V, Spinella-Jaegle S, Kawai S, Faucheu C, Huet L, Baron R, Roman-Roman S. Activation of mitogen-activated protein kinase cascades is involved in regulation of bone morphogenetic protein-2-induced osteoblast differentiation in pluripotent C2C12 cells. Bone. 2001; 28:491–8. [PubMed: 11344048]

[57]. Greenblatt MB, Shim JH, Zou W, Sitara D, Schweitzer M, Hu D, Lotinun S, Sano Y, Baron R, Park JM, Arthur S, et al. The p38 MAPK pathway is essential for skeletogenesis and bone homeostasis in mice. J Clin Invest. 2010; 120:2457–73. [PubMed: 20551513]

[58]. Heining E, Bhushan R, Paarmann P, Henis YI, Knaus P. Spatial segregation of BMP/Smad signaling affects osteoblast differentiation in C2C12 cells. PLoS One. 2011; 6:e25163. [PubMed: 21998639]

[59]. Nassoy P, Lamaze C. Stressing caveolae new role in cell mechanics. Trends Cell Biol. 2012; 22:381–9. [PubMed: 22613354]

[60]. Cheng JP, Nichols BJ. Caveolae: One function or many? Trends Cell Biol. 2016; 26:177–89. [PubMed: 26653791]

[61]. Sinha B, Koster D, Ruez R, Gonnord P, Bastiani M, Abankwa D, Stan RV, Butler-Browne G, Vedie B, Johannes L, Morone N, et al. Cells respond to mechanical stress by rapid disassembly of caveolae. Cell. 2011; 144:402–13. [PubMed: 21295700]

[62]. Bonor J, Adams EL, Bragdon B, Moseychuk O, Czymmek KJ, Nohe A. Initiation of BMP2 signaling in domains on the plasma membrane. J Cell Physiol. 2012; 227:2880–8. [PubMed: 21938723]

[63]. Nohe A, Keating E, Underhill TM, Knaus P, Petersen NO. Dynamics and interaction of caveolin-1 isoforms with BMP-receptors. J Cell Sci. 2005; 118:643–50. [PubMed: 15657086]

[64]. Rauch C, Brunet AC, Deleule J, Farge E. C2C12 myoblast/osteoblast transdifferentiation steps enhanced by epigenetic inhibition of BMP2 endocytosis. Am J Physiol Cell Physiol. 2002; 283:C235–43. [PubMed: 12055092]

[65]. Urrutia R, Henley JR, Cook T, McNiven MA. The dynamins: redundant or distinct functions for an expanding family of related GTPases? Proc Natl Acad Sci U S A. 1997; 94:377–84. [PubMed: 9012790]

[66]. van der Bliek AM. Functional diversity in the dynamin family. Trends Cell Biol. 1999; 9:96–102. [PubMed: 10201074]

[67]. Paarmann P, Dorpholz G, Fiebig J, Amsalem AR, Ehrlich M, Henis YI, Muller T, Knaus P. Dynamin-dependent endocytosis of Bone Morphogenetic Protein2 (BMP2) and its receptors is dispensable for the initiation of Smad signaling. Int J Biochem Cell Biol. 2016; 76:51–63. [PubMed: 27113717]

[68]. Marom B, Heining E, Knaus P, Henis YI. Formation of stable homomeric and transient heteromeric bone morphogenetic protein (BMP) receptor complexes regulates Smad protein signaling. J Biol Chem. 2011; 286:19287–96. [PubMed: 21471205]

[69]. Schwab EH, Pohl TL, Haraszti T, Schwaerzer GK, Hiepen C, Spatz JP, Knaus P, Cavalcanti-Adam EA. Nanoscale control of surface immobilized BMP-2: toward a quantitative assessment of BMP-mediated signaling events. Nano Lett. 2015; 15:1526–34. [PubMed: 25668064]

[70]. Dai J, Ting-Beall HP, Sheetz MP. The secretion-coupled endocytosis correlates with membrane tension changes in RBL 2H3 cells. J Gen Physiol. 1997; 110:1–10. [PubMed: 9234166]

[71]. Saleem M, Morlot S, Hohendahl A, Manzi J, Lenz M, Roux A. A balance between membrane elasticity and polymerization energy sets the shape of spherical clathrin coats. Nat Commun. 2015; 6:6249. [PubMed: 25695735]
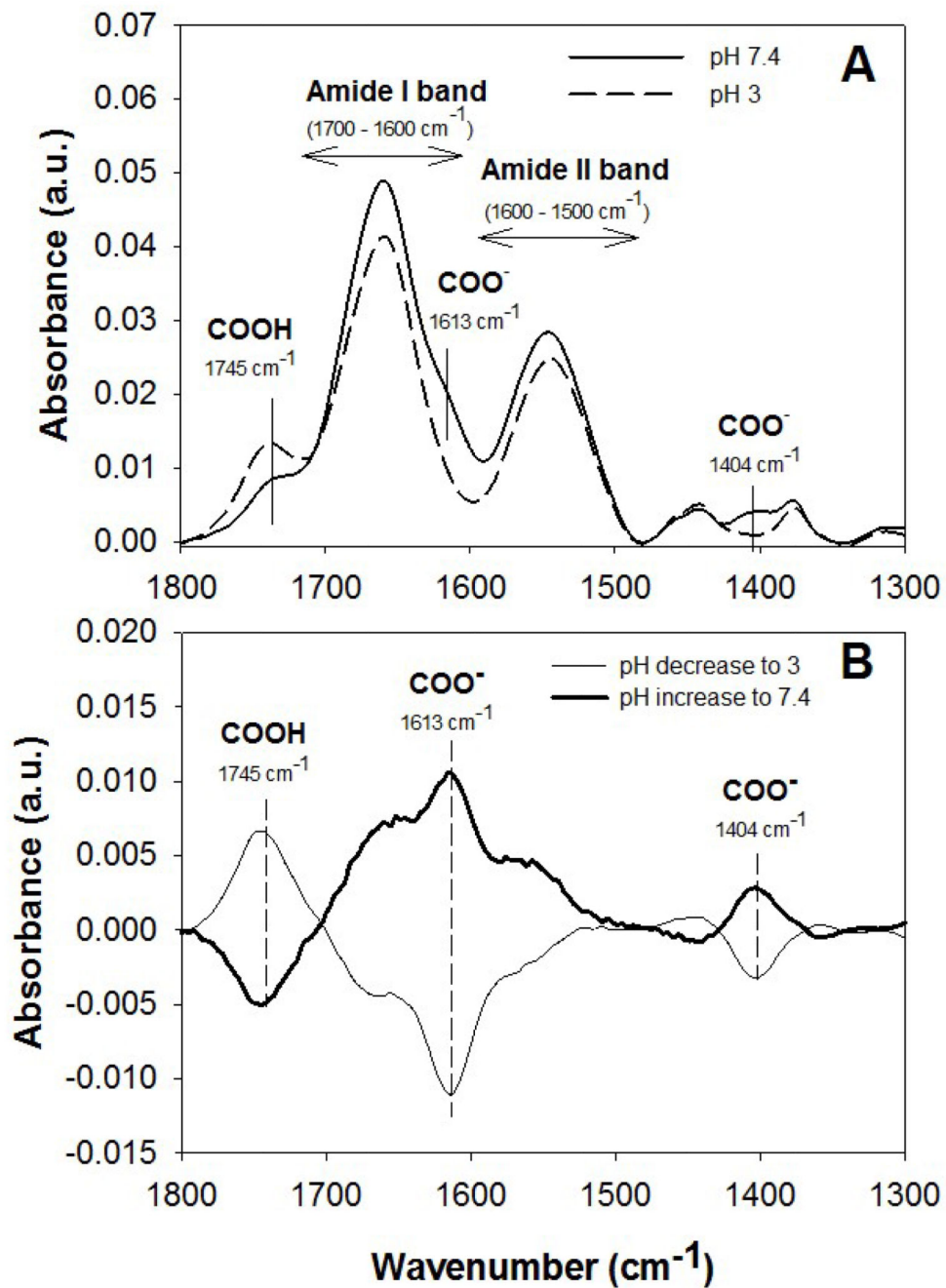
Figure 1. Effect of pH change on the infrared spectrum of the film.
(A) FTIR spectra of a $(PLL/HA)_{12}$ film before and after rinsing in 1 mM HCl (pH 3). (B) Subtraction between the spectrum before and after pH change gives the effect of the pH decrease (from 7.4 to 3) or of pH increase (from 3 to 7.4) in $(PLL/HA)_{12}$ films. The difference spectrum is the average of 6 different samples.
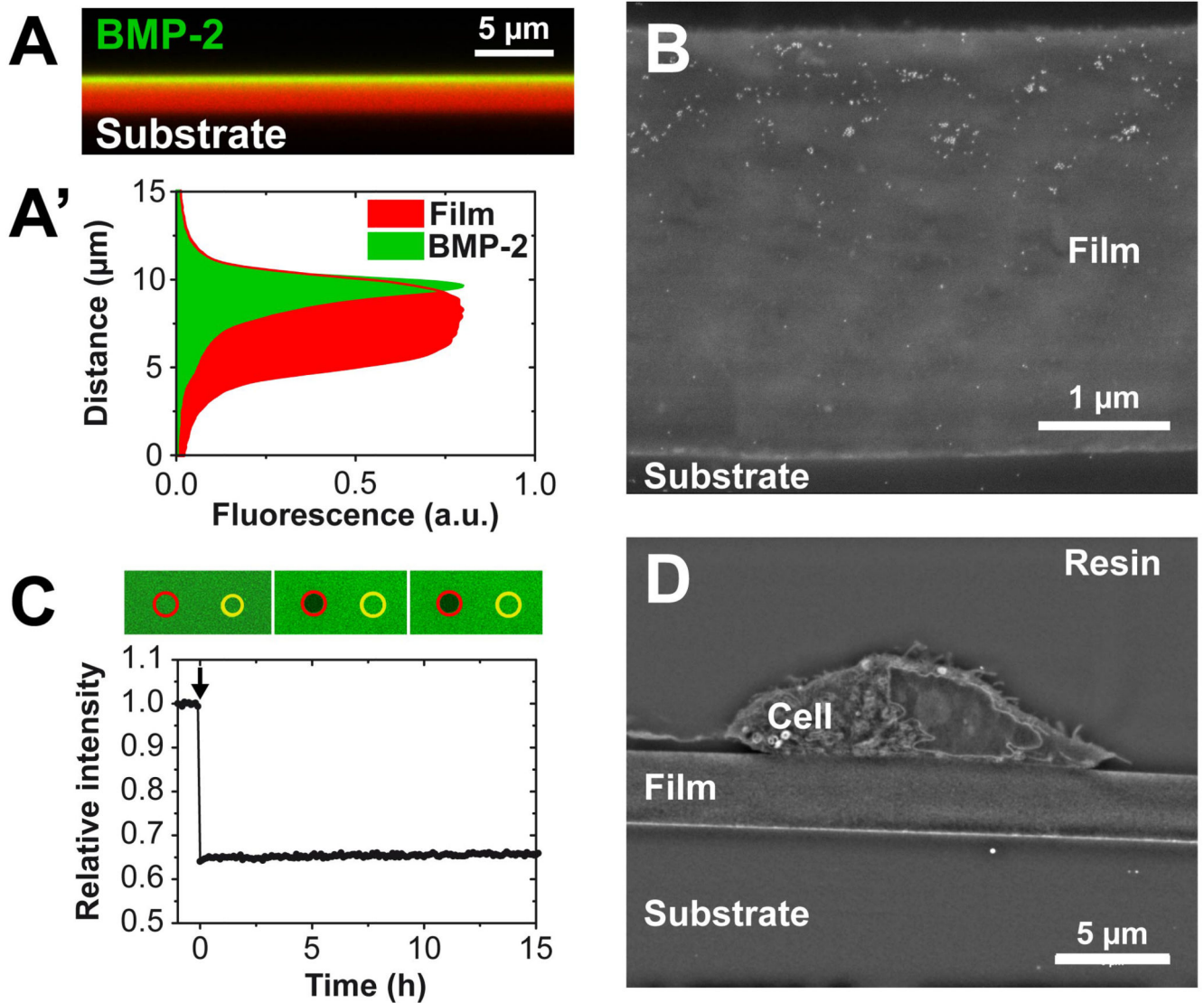
Figure 2. Visualization of BMP-2^{CF} trapping within a (PLL/HA)$_{24}$ film.
(A) Confocal image in XZ section of BMP-2^{CF} loaded inside a PLL-A568-labeled film (EDC10 film) (A') Fluorescence profile along the film thickness; (B) SEM image of a film cross-section (EDC10 films) after immunogold labeling of BMP-2; the white dots are 10 nm diameter gold nanoparticles; (C) Fluorescence recovery after photobleaching of BMP-2^{CF} inside a film crosslinked at EDC 10. (D) SEM image of a cross-section of a C2C12 cell seeded on top of a film after 24 h of culture.
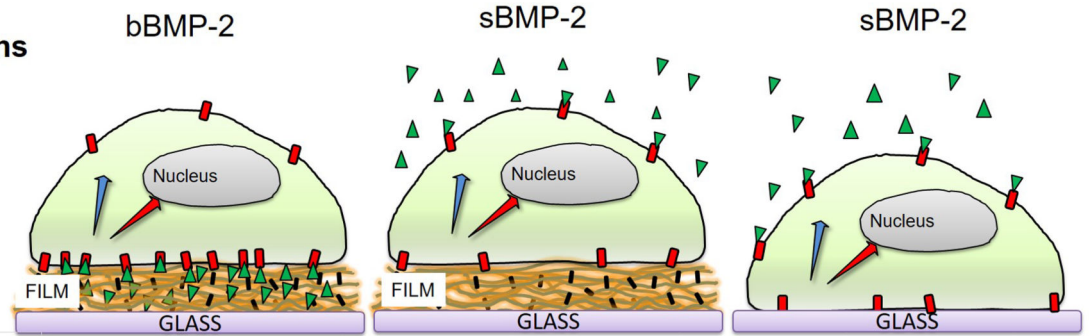
Figure 3. Schematic showing the differences in BMP-2 presentation mode: localized delivery at the ventral side of a cell for bBMP-2, or dorsal side for sBMP-2.
Cells are lying on top of the film or directly on glass. The characteristics of the presentation mode, BMP-2 lifetime, diffusion and the type of BMP2/BMPR interactions (basal or ventral side) are given.
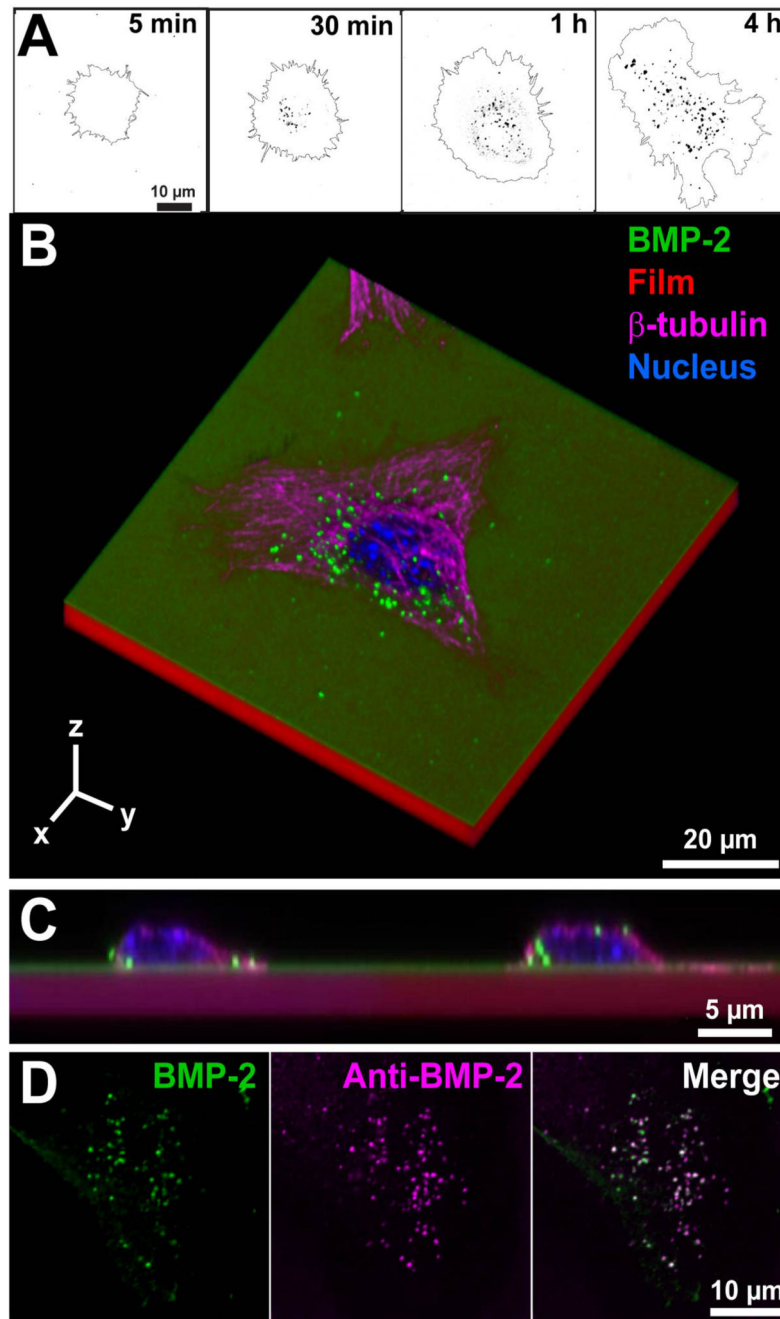
Figure 4. Confocal imaging of the uptake of matrix-bound BMP-2^{CF} by C2C12 cells.
(A) Confocal images of internalized bBMP-2^{CF} after 5 min, 30 min, 1h or 4h of cell contact with the EDC 10 film. The images represent the vesicles containing BMP-2 as dark spots and the cell contour. Scale bar: 10 μm (B) 3D representation of a C2C12 cell on top of a BMP-2^{CF} loaded film after 4h of culture (image size is 80 x 80 x 12 μm);(C) Cross-section of C2C12 cells on a bBMP-2 film after internalization of BMP-2^{CF} ; the films were labelled with PLL-A568 and cells were stained for their nucleus and actin cytoskeleton (D) Co-

staining of BMP-2^{CF} (green) inside vesicles with an anti-BMP-2 antibody (purple), as well as merge of the two images.
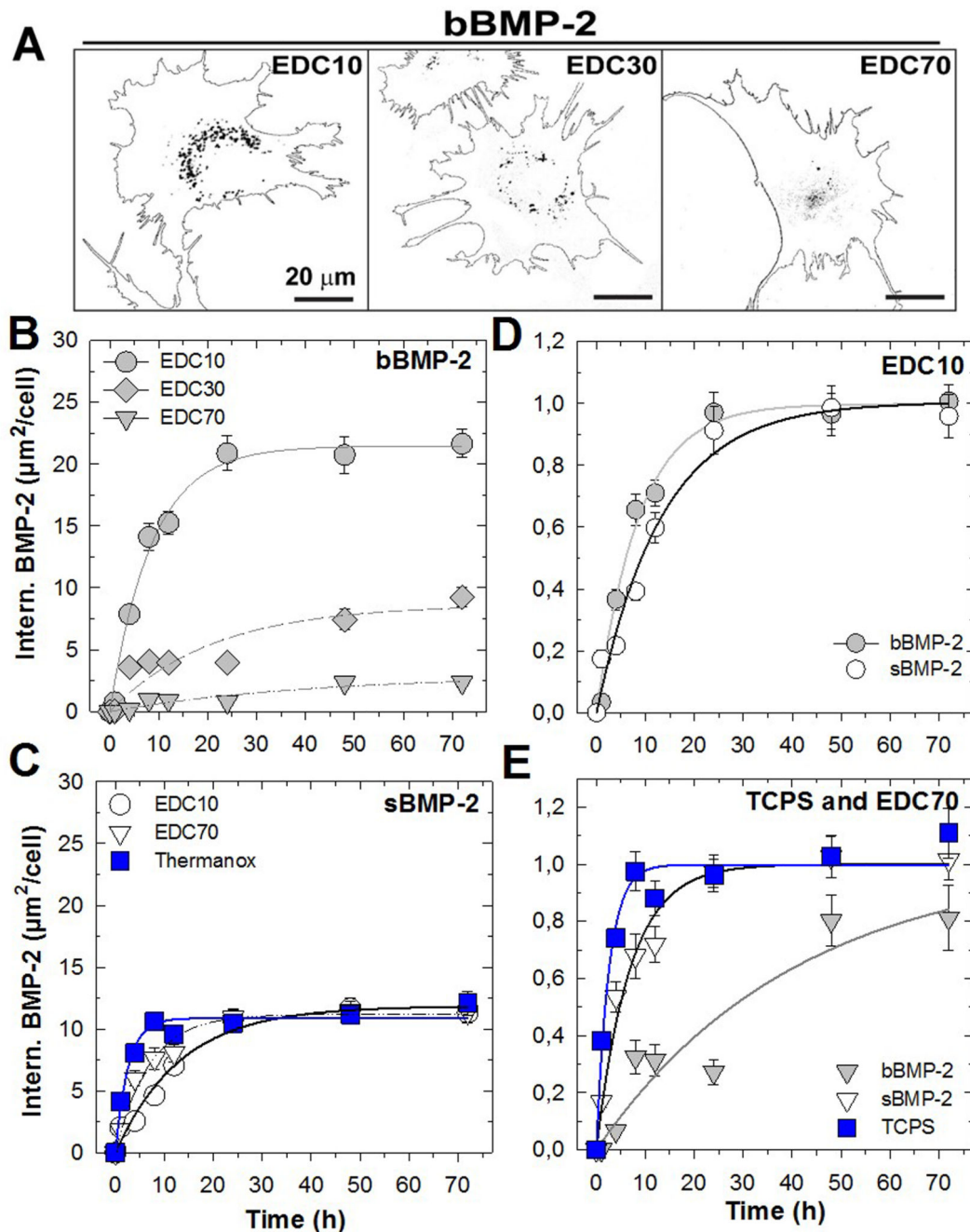
Figure 5. Internalization of matrix-bound and soluble BMP-2 over 3 days in function of film crosslinking.

(A) Confocal images of internalized bBMP-2^{CF} (cell contours and BMP-2 as dark spots) from films crosslinked to different extents (EDC10, 30 and 70). (B,C) Quantification of the internalized amounts over time, from 1h to 3 days for (B) bBMP-2 and (C) sBMP-2 on the different matrices (EDC10, EDC70 and TCPS). Internalization over time after normalization, for each experimental condition, to its plateau value (values taken from Table 1); (D) for EDC10 with sBMP-2 and bBMP-2; (E) for EDC70 and Plastic. Data are mean ±

SEM of the mean for three independent experiments. For each experiment, 100 cells were analyzed per condition.
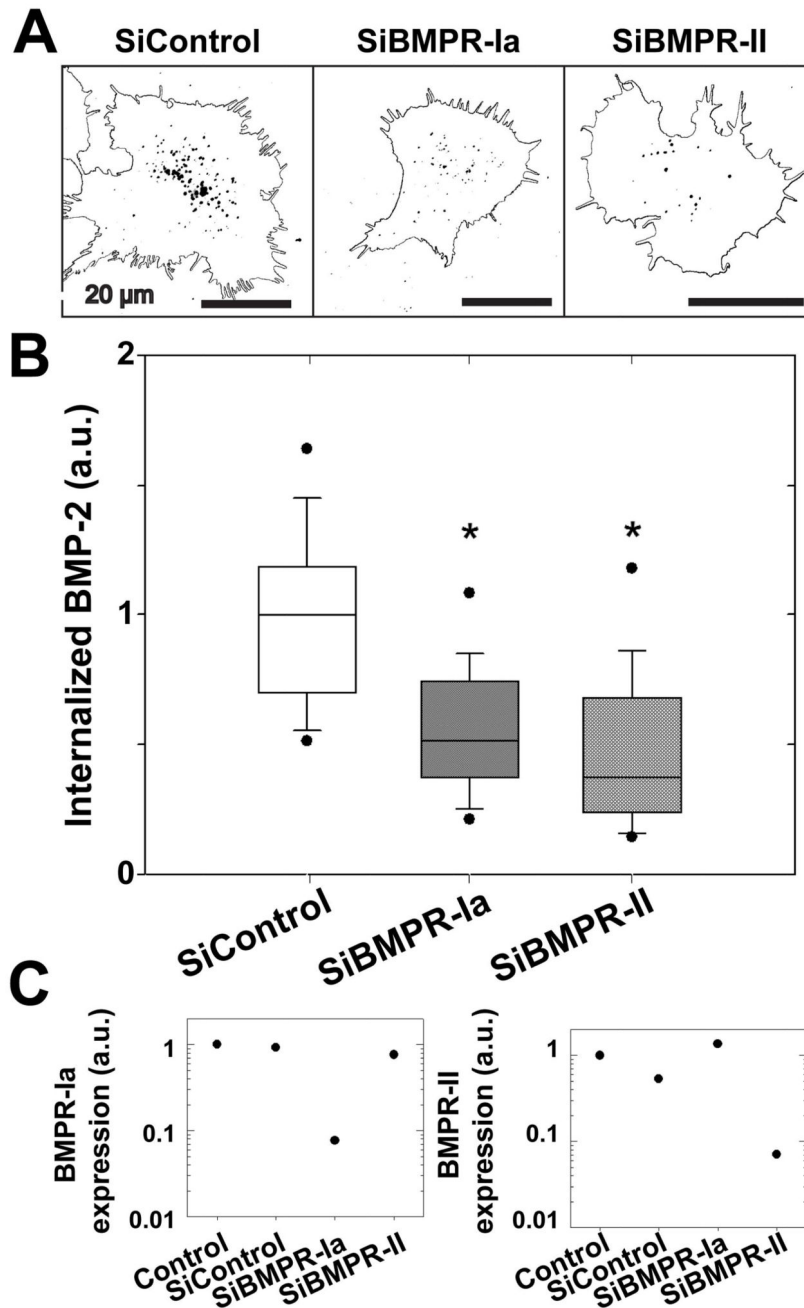
Figure 6. Role of BMP receptors in the internalization of matrix-bound bBMP-2.
(A) Representative images of the cells (cell contour and internalized BMP-2 as dark spots) with knockdown of BMPR-IA and BMPR-II receptors after 4 h of culture on EDC10 films; (B) Quantification of the internalized amount of bBMP-2^{CF} after transfection. The total amount of BMP-2 per cell was calculated for each cell. Data are represented as box plots for 70 cells per condition and normalized to SiControl (C) Efficacy of the SiRNA against receptors as assessed by qPCR. *p<0.001.
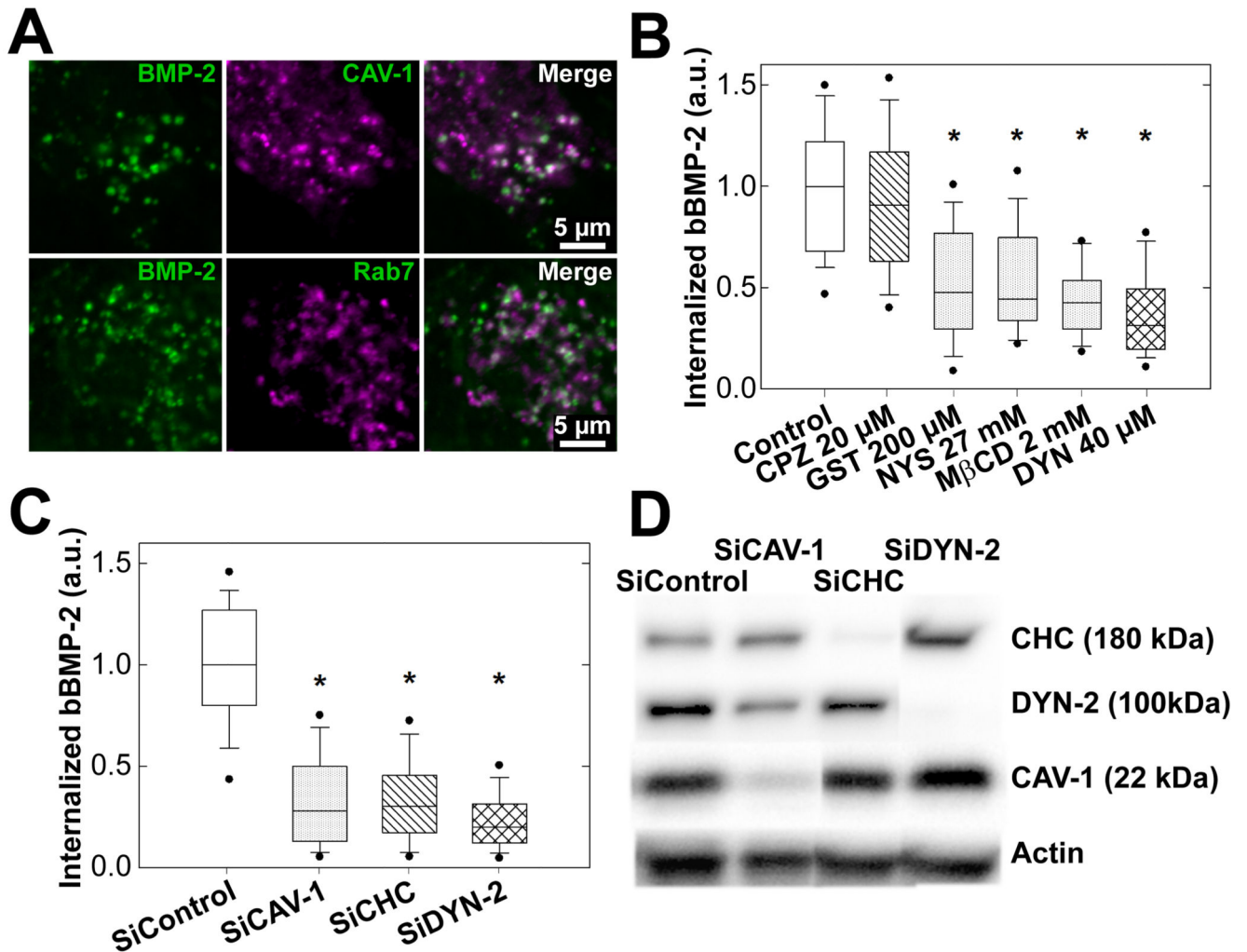
Figure 7. Internalization route of matrix-bound BMP-2.

(A) Confocal images showing colocalization of BMP-2^{CF} vesicles with the endocytic markers Cav-1 and rab7 after 8 h of culture (scale bar 5 μm). (B) Effect of different inhibitors, 20 μM CPZ, 200 μM GST, 27 mM NYS, 2 mM MβCD and 40 μM DYN on bBMP-2 internalization; (C) Effect of siRNA-mediated knockdown of endocytic proteins on bBMP-2^{CF}internalization. For (C) and (D), data are pooled from three independent experiments after normalization to the SiControl condition, with 70 cells analyzed for each condition in each experiment (D) Efficacy of the siRNA against CHC, CAV-1 and DYN-2 was confirmed by Western blot analysis.*p<0.001
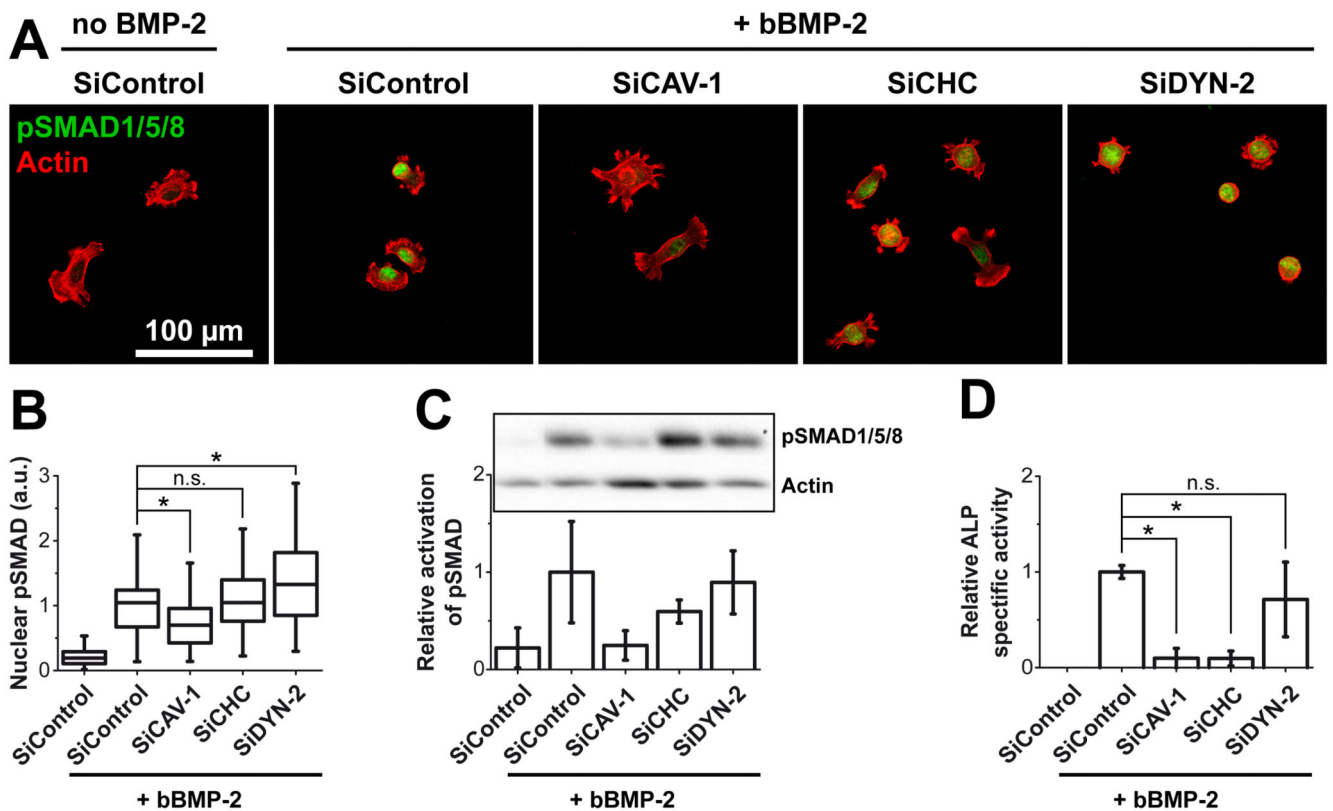
Figure 8. Effect of the inhibition of endocytosis on the signaling pathway of matrix-bound BMP-2 using specific knockdown of endocytic proteins

(same siRNA against CAV-1, CHC and DYN-2 as in Figure 7.) (A) Fluorescence images of pSMAD (green) and actin (red) for the different SiRNAs and (B) Quantification of the amount of nuclear pSMAD; the median value for siControl is normalized to 1; the analyses were made on more than 70 cells for each condition, in duplicate samples.(C) Quantitative expression of pSMAD by Western blotting; data represent mean ± SD of three independent experiments, with one sample per condition in each experiment (data being normalized by the band of actin) (D) Relative ALP activity after 3 days after protein knockdown. Data correspond to mean ± SD of three independent experiments, with three samples per condition in each experiment. * p< 0.01
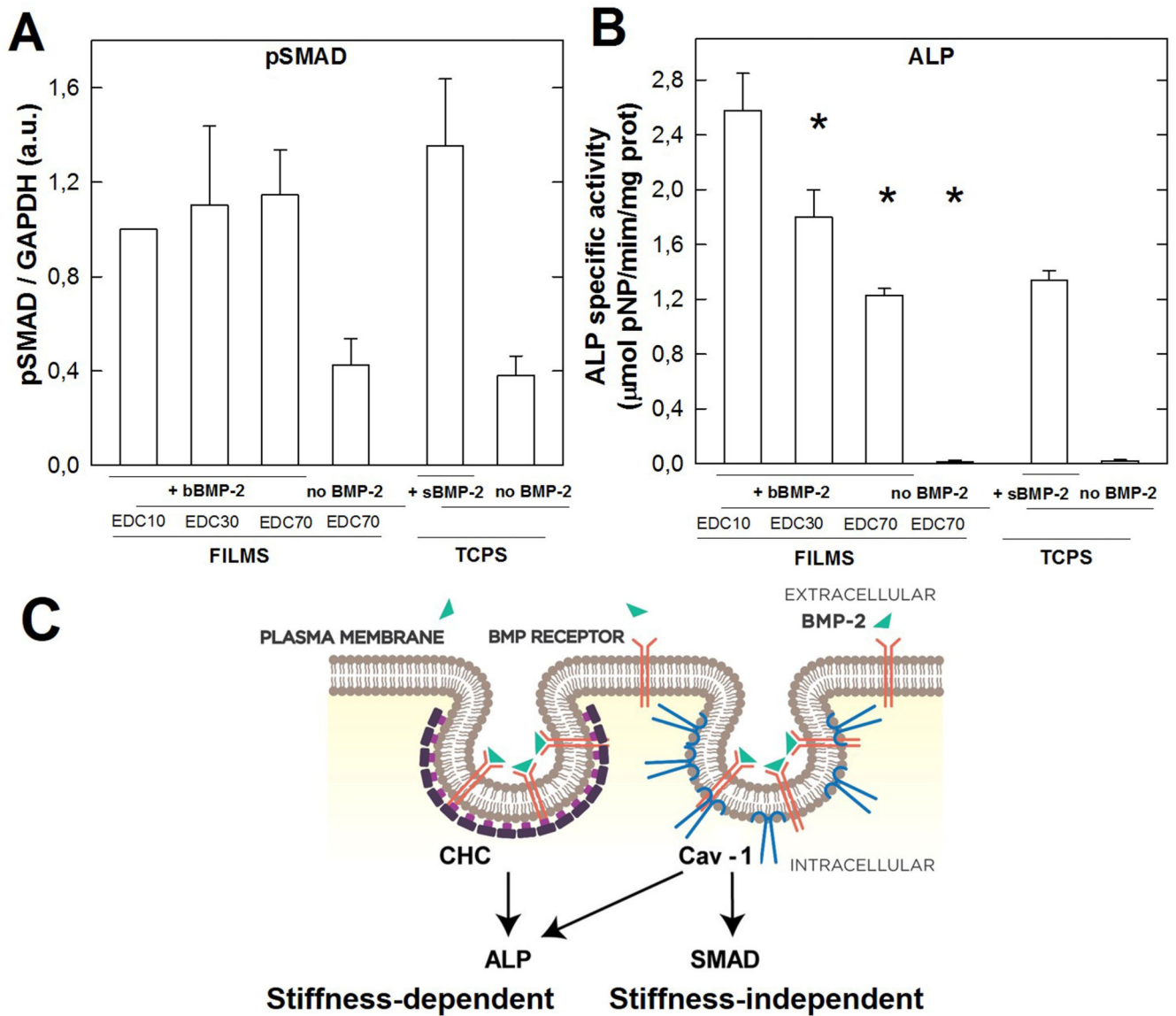
Figure 9. Coupling between endocytosis and signaling.

The signaling was assessed by the quantification of pSMAD by Western blotting (A) and ALP activity (B) for the films of different crosslinking levels. For pSMAD, GADPH was taken as reference to normalize the signal for each experimental condition. Data are mean ± SD of two independent experiments with two independent samples per condition in each experiment. **(C)** Summary scheme: Cav-1 mediates both SMAD and ALP signaling while CHC mediates only ALP signaling. In our experimental conditions, ALP is stiffness-dependent while pSMAD is stiffness-independent. ***** $p < 0.01$

Table 1

Internalized amount reached at the plateau value (I_{max}) and characteristic internalization time (τ) deduced from the fitting of the experimental curves of Fig. 3A' and Fig. B', i.e. internalized amount of BMP-2-containing vesicles for bBMP-2 and sBMP-2.

	bBMP-2			sBMP-2		
	I_{max} (µm²/cell)	τ (h)	R	I_{max} (µm²/cell)	τ (h)	R
EDC 10	21.5 ± 0.6	8.6 ± 0.8	0.99	11.8 ± 0.6	13.3 ± 1.8	0.99
EDC 30	8.7 ± 1.5	20.8 ± 8.8	0.92	---	---	---
EDC 70	2.9 ± 0.8	40.7 ± 21.5	0.95	11.2 ± 0.4	6.9 ± 0.9	0.99
Thermanox	-	-	-	10.9 ± 0.4	2.6 ± 0.5	0.98